ResearchGate

See discussions, stats, and author profiles for this publication at: https://www.researchgate.net/publication/234061950

Synthesis, Characterization, Reactivity, and Linkage Isomerization of Ru(Cl) 2 (L)(DMSO) 2 Complexes

ARTICLE *in* BERICHTE DER DEUTSCHEN CHEMISCHEN GESELLSCHAFT · JANUARY 2013

Impact Factor: 2.94 · DOI: 10.1002/ejic.201200809

CITATIONS
4

READS
43

5 AUTHORS, INCLUDING:

Somnath Maji
Indian Institute of Technology Hyderabad
37 PUBLICATIONS **593** CITATIONS

SEE PROFILE

Josefina Pons
Autonomous University of Barcelona
162 PUBLICATIONS **2,510** CITATIONS

SEE PROFILE

Antoni Llobet
ICIQ Institute of Chemical Research of Catal…
196 PUBLICATIONS **5,253** CITATIONS

SEE PROFILE

Available from: Somnath Maji
Retrieved on: 24 January 2016

EurJIC European Journal of Inorganic Chemistry

ChemPubSoc Europe

FULL PAPER

DOI:10.1002/ejic.201200809

Synthesis, Characterization, Reactivity, and Linkage Isomerization of $Ru(Cl)_2(L)(DMSO)_2$ Complexes

Stephan Roeser,*[a] Somnath Maji,[a] Jordi Benet-Buchholz,[a] Josefina Pons,[b] and Antoni Llobet*[a,b]

Keywords: Redox chemistry / Isomerization / Ruthenium

The structures, spectroscopic properties, electrochemistry, and reactivity of two new isomeric $[Ru(Cl)_2(L)(DMSO)_2]$ complexes are reported [L is the nonsymmetric chelating ligand 5-phenyl-3-(2-pyridyl)-1*H*-pyrazole (H3p), DMSO = dimethyl sulfoxide]. It is shown that there is S-to-O linkage isomerization of the ruthenium(II) sulfoxide complexes upon one electron oxidation. The thermodynamic and kinetic properties of this linkage isomerization differ for each isomeric complex and depend strongly on the protonation grade of the ligand backbone. The corresponding data for these processes were evaluated from electrochemical data. A photolytic reaction of either of these isomers in chloroform is presented and leads to the substitution of one DMSO ligand and the formation of a third complex, $[Ru(Cl)_3(L)(DMSO)]$. The remaining coordinated DMSO ligand retains its binding mode through the sulfur atom to a ruthenium(III) metal center.

Introduction

Since the introduction of $[Ru(Cl)_2(DMSO)_4]$ (DMSO = dimethyl sulfoxide) by Wilkinson et al. in 1973,[1] a huge number of ruthenium compounds containing DMSO ligands combined with a variety of auxiliary ligands have been described. These complexes are an interesting class of compounds for a variety of reasons. Some have antitumor[2] and radio sensitizing properties[3] and some have been used as catalyst precursors in several processes. Among these are key reactions such as air oxidation of thioethers to sulfoxides[4] and of sulfoxides to sulfones,[5] hydrogenolysis of O_2 to H_2O_2,[6] polymerization of olefins[7] and cyclic olefins,[8] as well as isomerization of allylic alcohols.[9] Another important characteristic of these complexes is their ability to undergo light-[10] or electron-transfer-induced conformational changes.[11] This property is crucial to the operation of molecular machines and to other types of molecular bistability[12] and has possible use in information storage devices.[13] The focus of this study is on the synthesis of a pair of isomeric ruthenium(II) complexes, their thorough characterization, and a comparison of their different tendencies towards electron-transfer-induced linkage isomerization of the DMSO ligand. Furthermore, we report the reactivity of both isomers towards light irradiation in $CHCl_3$, which leads to the formation of a Ru^{III} complex, $[RuCl_3(L)(DMSO)]$, in which the remaining DMSO ligand coordinates through its sulfur atom rather than through the expected oxygen atom.

[a] Institute of Chemical Research of Catalonia (ICIQ), Avinguda Països Catalans 16, 43007 Tarragona, Spain
E-mail: stephan.roeser@gmail.com
Homepage: http://www.iciq.es/portal/mid!447/ModeID!0/EhPageID!120958/351/Default.aspx
[b] Departament de Química, Universitat Autonoma de Barcelona, 08193 Bellaterra, Spain
E-mail: allobet@iciq.es
Homepage: http://www.iciq.es/portal/351/default.aspx
Supporting information for this article is available on the WWW under http://dx.doi.org/10.1002/ejic.201200809.

Results and Discussion

Synthesis, Structure, and Stereoisomerism

The equimolar reaction of 5-phenyl-3-(2-pyridyl)-1*H*-pyrazole (H3p) with *cis*-$[Ru(Cl)_2(DMSO)_4]$ in refluxing methanol and in the absence of light results in the preferential formation of one out of six possible isomers (including the two possible pairs of enantiomers, Scheme 1) within 45 min, namely, the C_s-symmetric complex *trans,cis*-$[Ru(Cl)_2(H3p)(DMSO)_2]$ (**1a**,). Complex **1a** can be easily isolated by filtration in 70% yield. The composition of the filtrates, revealed by ^1H NMR experiments, consists mainly of **1a** plus another isomeric compound, to be exact the C_1 symmetric complex *cis(out),cis(in)*-$[Ru(Cl)_2(H3p)(DMSO)_2]$ (**1b**, see Supporting Information).

Complex **1b** was obtained as the main product in good yield (75%) when the reaction time was prolonged to 18 h (Scheme 2) and was again easily isolated by filtration owing to its insolubility in the reaction solvent. Effectively, the yield is almost quantitative, which could be demonstrated by ^1H NMR experiments on the mother solution (see Supporting Information). Concerning the nomenclature of the complexes, the prefix (*out*)- relates to the chlorido ligand that is coplanar with the coordinated H3p ligand and *trans*

 © 2013 Wiley-VCH Verlag GmbH & Co. KGaA, Weinheim

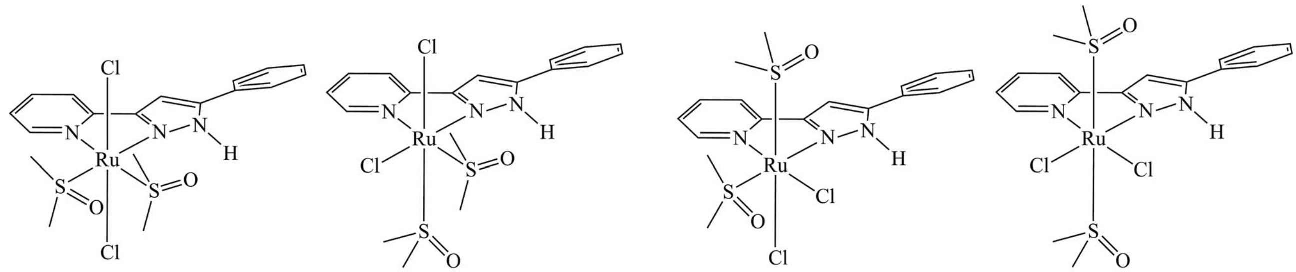

cis-DMSO, *trans*-chlorido (**1a**) *Λ-cis(in)*-DMSO, *cis(out)*-chlorido (**1b**) *Λ-cis(out)*-DMSO, *cis(in)*-chlorido (**1c**) *trans*-DMSO, *cis*-chlorido (**1d**)

Scheme 1. Possible stereoisomers for [Ru(Cl)$_2$(H3p)(DMSO)$_2$].

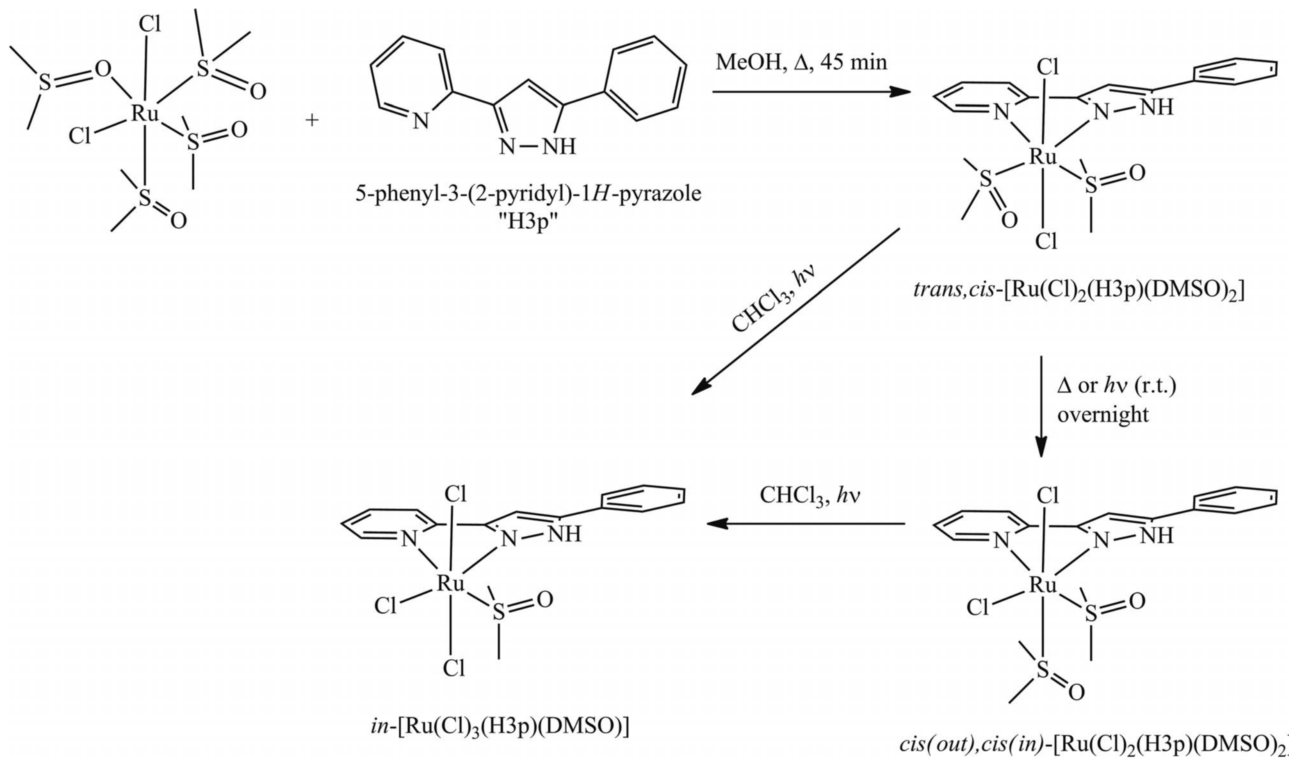

Scheme 2. Synthetic strategies for the preparation of **1a**, **1b**, and **2**.

to the pyrazole moiety. The prefix (*in*)- denotes the orientation of the coplanar DMSO ligand, which is *trans* to the pyridine group, towards the pyrazole group.

We propose that the formation of **1a** as the major kinetic product is followed by isomerization to the thermodynamically most stable complex, **1b**. An attempt to follow this thermally induced isomerization of **1a** in [D$_6$]DMSO by ^{1}H NMR spectroscopy failed, as even after 4 h at 45 °C no sign of **1b** could be observed. This observation hints towards the possibility that isomerization initiates through decoordination of the DMSO ligand. In neat DMSO this step would be disfavored and therefore no isomerization would occur. In contrast, almost complete transformation was obtained after 7 h in the same solvent by using a 200 W Tungsten lamp (and keeping the temperature constant at 28 °C, see Supporting Information), which suggests a different reaction pathway that is thermally not accessible. Control experiments for the thermal induced isomerization in [D$_4$]-MeOH were unsuccessful due to the insolubility of **1a** in this solvent.

On irradiating a sample of **1a** or **1b** in freshly distilled CHCl$_3$, a color change from bright yellow to deep red was observed. This spectral change (Figure 3) could be assigned to a substitution reaction of one DMSO ligand by a chlorido ligand. This substitution is accompanied by a change in oxidation state to Ru^{III} and the formation of **2**, *in*-[Ru(Cl)$_3$(H3p)(DMSO)]. The prefix *in*- of **2** refers to the position of the remaining coordinating DMSO as described above.

The photoinduced decomposition of CHCl$_3$ in the presence of a Ru^{II} compound has been observed before.[14] This reaction occurred through initial C–Cl bond homolysis of CHCl$_3$ by UV light absorption in deoxygenated solvent.

To unravel the influence of our Ru^{II} compound on this reaction, a variety of cut-off filters were applied. Although both isomers lead to the formation of the same product,

 © 2013 Wiley-VCH Verlag GmbH & Co. KGaA, Weinheim

1b was chosen for this particular investigation so that any possible influence of isomerization processes could be discarder. Upon irradiation of the complex with light ($\lambda \geq$ 375 nm) that excites only low energy metal-to-ligand charge transfer (MLCT) transitions, no reaction occurs (see Supporting Information). To our surprise, the same change in absorption using no filter can be observed in a comparable overall velocity by applying a cutoff filter at 305 nm. It should be noted that this excitation wavelength is cut-off around 40 nm over the absorption limit of the solvent. Therefore, the reaction is not initiated by the bond homolysis of the solvent $CHCl_3$, but rather is promoted by high-energy transitions of the compound itself. In addition, this reaction does not depend on the presence or absence of oxygen (see Supporting Information).

From crystallographic data, it could be seen that in both cases the outer DMSO ligand of **1a** and the axial one of **1b** is substituted selectively. This might be due to the stabilizing hydrogen bond of the oxygen atom O(1) of the inner DMSO ligand with the pyrazolic hydrogen [HN(3), see Figure 1). The crystallographic data for **1a**, **1b**, and **2** are presented in Table 1.

ORTEP plots of the molecular structures of **1a**, **1b**, and **2** are depicted in Figure 1. Their metal–ligand bond lengths are similar to those of complexes previously reported.[15] Of most interest are the bond lengths of the coordinated DMSO ligand(s) in **1a**, **1b**, and **2**. In **1a** as well as in **1b** there are two DMSO ligands present, which differ in their Ru–S bond lengths [Ru–S(1) 2.2584(11), 2.2419(12) Å; Ru–S(2) 2.2684(12), 2.2670(12) Å (**1a**); Ru–S(1) 2.2518(15) Å; Ru–S(2) 2.2343(14) Å (**1b**)] and in their S–O bond lengths [S(1)–O(1) 1.493(4), 1.499(4) Å; S(2)–O(2) 1.482(4), 1.472(4) Å (**1a**); S(1)–O(1) 1.491(4) Å; S(2)–O(2) 1.479(4) Å (**1b**)]. The coordinated DMSO(2) ligand in **1a** and DMSO(2) ligand in **1b** have shorter S–O bond lengths than those of free DMSO [1.492(1) Å],[16] which is attributed to a higher degree of S–O double bond character. In **2**, the Ru(1)–S(1) bond length is 2.2655(2) Å and the S(1)–O(1) bond length is 1.4910(16) Å. This suggests that the DMSO(2) ligand in **1a** and the DMSO(2) ligand in **1b** act primarily as σ-donor ligands. The contracted Ru–S bond of the DMSO(1) ligand in **1a** and the DMSO(2) ligand of **1b** most likely arise from π back bonding from the Ru atom.

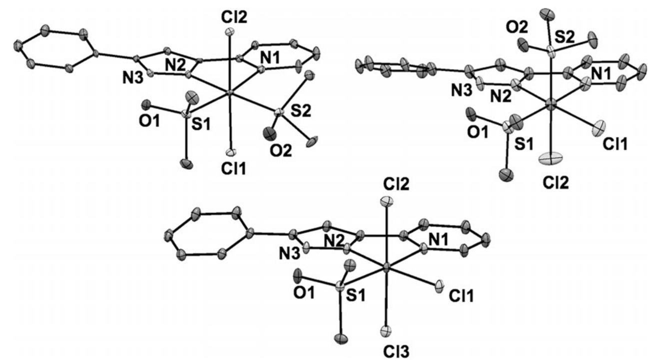

Figure 1. ORTEP plots of the molecular structures (ellipsoids at 30% probability) of *trans,cis*-[Ru(Cl)$_2$(H3p)(DMSO)$_2$], (**1a**, top left), *cis(out),cis(in)*-[Ru(Cl)$_2$(H3p)(DMSO)$_2$], (**1b**, top right) and *in*-[Ru(Cl)$_3$(H3p)(DMSO)], (**2**, bottom). For clarity, carbon atoms are not labeled and hydrogen atoms are not shown.

In the pseudo-octahedral coordination of the Ru atom of **1a**, the chlorido ligands are in *trans* positions and present a Cl(1)–Ru–Cl(2) angle of 179.62–179.95°, which is only slightly smaller than that in an ideal octahedral coordination. A more drastic difference from ideal coordination is represented by the acute bite angle of 75.96, 76.09° of N(2)–Ru–N(1), which is caused by the chelate coordination of the H3p ligand. Consequently, all other angles in this plane are larger than 90°. The interaction of HN(3) with the oxygen atom of the inner DMSO(2) ligand {N(3)–O(2) 2.669, 2.699 Å, ∠[O(2)–H–N(3)] 134.83, 134.85°} produces a N(2)–Ru–S(2) angle of 92.03, 92.88°, which is close to the ideal 90°. The hydrogen bond interaction is mainly of electrostatic nature and of medium strength with a relatively large N(3)–H–O(2) bond angle of at least 130° and a relatively long N(3)···O(2) distance of at least 2.5 Å.[17] This interaction induces the methyl groups of the DMSO(2) li-

Table 1. Crystallographic data for complexes **1a**, **1b**, and **2**.

Complex	1a	1b	2
Empirical formula	$C_{38}H_{48}Cl_{10}N_6O_4Ru_2S_4$	$C_{38}H_{48}Cl_{10}N_6O_4Ru_2S_4$	$C_{17}H_{18}Cl_6N_3ORuS$
FW [g/mol]	1337.70	1337.70	626.17
Crystal system, space group	monoclinic, *Cc*	monoclinic, *C*2/*c*	triclinic, $P\bar{1}$
a [Å]	30.156(2)	30.419(3)	10.3226(6)
b [Å]	13.2566(9)	8.3313(11)	10.9634(5)
c [Å]	13.0227(9)	23.670(3)	11.8960(6)
α [°]	90	90	93.623(2)
β [°]	90.548(2)	120.110(5)	107.575(2)
γ [°]	90	90	110.472(2)
V [Å^3]	5205.8(6)	5189.3(11)	1180.71(11)
Formula units/cell	4	4	2
T [K]	100(2)	100(2)	100(2)
λ (Mo-K_α) [Å]	0.71073	0.71073	0.71073
ρ_{calc}, g/cm^3	1.707	1.712	1.761
μ [mm^{-1}]	1.299	1.303	1.446
R indices [$I > 2\sigma(I)$]	R_1 = 0.0441, $wR2$ = 0.1202	R_1 = 0.0802, $wR2$ = 0.1708	R_1 = 0.0361, $wR2$ = 0.0939
R indices (all data)	R_1 = 0.0483, $wR2$ = 0.1235	R_1 = 0.1136, $wR2$ = 0.1870	R_1 = 0.0431, $wR2$ = 0.0990

 © 2013 Wiley-VCH Verlag GmbH & Co. KGaA, Weinheim

gand to point above and below the equatorial plane described by N(1)–N(2)–S(2)–S(1). This again has a direct effect on the conformation of the second DMSO(1) ligand, which points with its O(1) atom towards the spatial center of the two methyl groups of DMSO(2) and has the same arrangement of its two methyl groups as in DMSO(2).

Finally, the chelate coordination of the H3p ligand leads to a small torsion angle between the pyridyl and the pyrazole rings of around 2°. Slightly unexpectedly, the torsion angle between the pyrazole and the phenyl ring is only ca. 10°. From steric repulsion one would expect a 90° angle. Either packing in the crystal or electronic interactions between the phenyl and the pyrazole rings might account for this.[15b,18]

All the main structural features (chelating effect on coordination angles, intramolecular hydrogen bonding) of **1a** are found to a similar extent in the solid-state structures of **1b** and **2**. For **2**, the hydrogen-bond interaction between the inner DMSO ligand and the pyrazolic hydrogen atom (HN) provokes a rather unusual ligand coordination for Ru^{III}–sulfoxo complexes. Whereas the DMSO ligand normally switches from sulfur to oxygen atom coordination (linkage-bonding isomerization) upon oxidation,[13b,19] in **2** the DMSO ligand is coordinated through its sulfur atom. This characteristic has been reported before in related complexes with Ru^{III} coordinated by three chlorido ligands.[2c,20] Therefore, we propose that the strong σ-donating ability of the chlorido ligands weakens the Lewis acid character of the Ru^{III} metal center and hence the DMSO ligand prefers coordination through its softer S donor atom.

Spectroscopic and Photochemical Properties

Complete 1D and 2D NMR spectra are presented in the Supporting Information and throughout the manuscript. The ^{1}H NMR spectra of **1a** and **1b** in [D$_6$]DMSO with the corresponding assignations is shown in Figure 2. Both isomers could be identified unambiguously through ^{1}H NMR techniques. In solution the *trans,cis*-[Ru(Cl)$_2$(H3p)(DMSO)$_2$] complex **1a** is C_s-symmetric.

As a consequence, the two methyl groups of both DMSO ligands are magnetically identical and are represented in the ^{1}H NMR as two singlet peaks at δ = 3.45 and 3.48 ppm. Through intramolecular NOE interaction of the H_α atom of the pyridyl ring with both methyl groups of the outer DMSO ligand (δ = 3.45 ppm), one can easily assign these two peaks. In **1b** the C_s symmetry is broken and the two singlets for the methyl groups are split into four singlets. This implies that one DMSO ligand must occupy an equatorial and the other an axial coordination position. One can easily identify the position of the coordinated chlorido ligands in the ^{1}H NMR spectrum. In **1a** the deshielding effect of the free electron pair of a chlorido ligand causes the H_α atom of the pyridine ring to present a chemical shift of δ = 8.81 ppm, whereas in **1b** this signal is shifted significantly towards lower field to δ = 9.29 ppm. Therefore, the chlorido ligand must be in the equatorial *out* position. Having assigned the positions of the two chlorido ligands, one must only assign the four singlets to each DMSO ligand.

The equatorial DMSO ligand presents two singlets at δ = 2.21 and 2.95 ppm, which show strong coupling in a COSY-

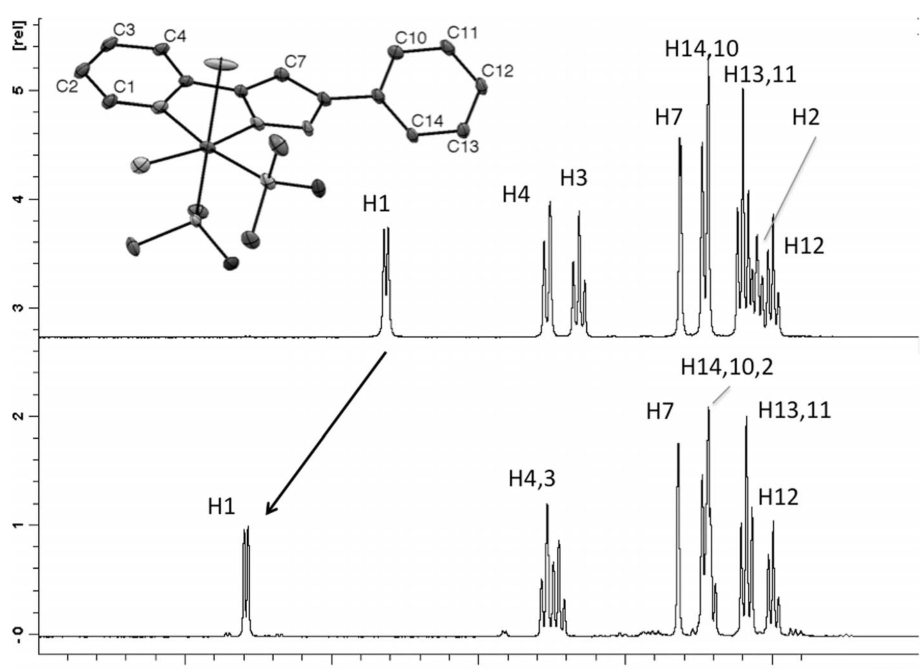

Figure 2. ^{1}H NMR spectra (aromatic region) and assignments for **1a** (top) and **1b** (bottom) recorded in [D$_6$]DMSO. Inset shows the crystal structure of **1b** with relevant labeling.

 © 2013 Wiley-VCH Verlag GmbH & Co. KGaA, Weinheim

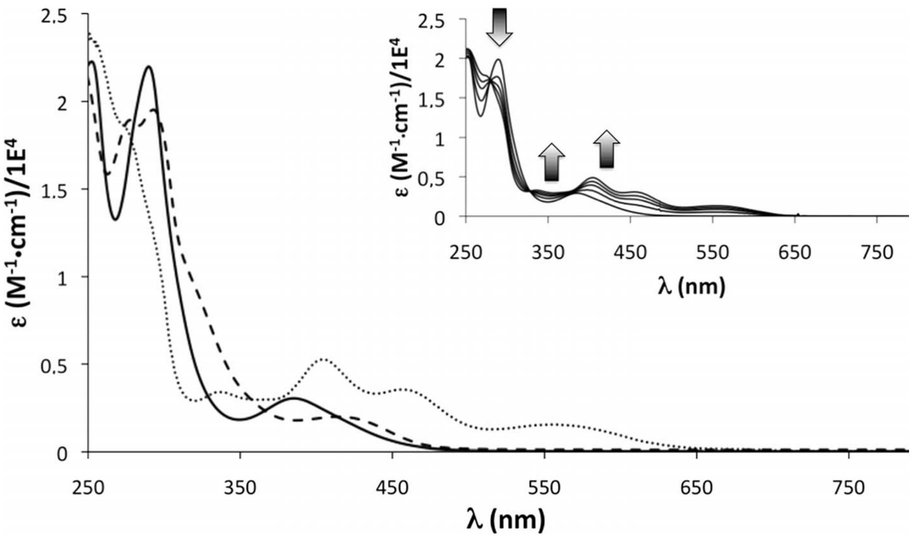

Figure 3. UV/Vis spectra of **1a** (solid), **1b** (dashed), and **2** (dotted) in $CHCl_3$. The inset shows the change in absorption during the photoinduced transformation of **1a** into **2** in $CHCl_3$.

NMR experiment. The orientation of this DMSO ligand is fixed by a hydrogen-bond interaction with the pyrazolic moiety. The difference in chemical shift can be explained by the deshielding effect of the free electron pair of the axial chlorido ligand. The two singlets at δ = 3.49 and 3.51 ppm are assigned to the methyl groups of the axially coordinated DMSO ligand, which presents signals at lower field owing to the anisotropic effect of the aromatic ring current of the H3p ligand.

The UV/Vis spectra of **1a**, **1b**, and **2** in $CHCl_3$ are presented in Figure 3. The absorption spectra of **1a** and **1b** are relatively alike. The absorption bands of $\lambda > 330$ nm can be assigned to $d\pi \rightarrow \pi^*$ (MLCT) transitions regarding the similarity of their transition energies and extinction coefficients with those of related complexes.[15a,21] An entirely different pattern of absorption bands was observed in **2**.

This difference is related to additional Cl $p\pi \rightarrow$ Ru $d\pi^*$ ligand-to-metal charge transfer (LMCT) transitions in the visible region.[20b] The major spectral features of **1a**, **1b**, and **2** are summarized in Table S1 (Supporting Information).

Redox Chemistry and Linkage Isomerization

The redox properties of the complexes presented here were investigated by cyclic voltammetry (CV). Typical plots are presented in Figure 4 and in the Supporting Information.

Complex **1a** presents a quasireversible wave for the $E_{1/2}$ of the Ru(III/II) redox couple at 0.94 V vs. sodium saturated calomel electrode (SSCE, $E_{p,a}$ = 0.98 V, $E_{p,c}$ = 0.90 V, ΔE = 80 mV). If the measurement is carried out in the presence of a base, the potential is lowered by 660 mV to 0.28 V ($E_{p,a}$ = 0.31 V, $E_{p,c}$ = 0.25 V, ΔE = 60 mV). This is in agreement with the following reaction occurring:

$$trans,cis\text{-}[Ru(Cl)_2(H3p)(DMSO)_2]\ (\mathbf{1a}) + t\mathrm{BuO}^- \rightarrow trans,cis\text{-}[Ru(Cl)_2(3p)(DMSO)_2]^-\ ([\mathbf{1a} - H]^-) + t\mathrm{BuOH} \quad (1)$$

The same behavior is observed with **1b**. In its protonated state, $E_{1/2}$ = 1.03 V ($E_{p,a}$ = 1.06 V, $E_{p,c}$ = 1.00 V, ΔE = 60 mV) for the redox couple Ru(III/II). Upon deprotonation, it shifts by 570 mV to 0.46 V ($E_{p,a}$ = 0.52 V, $E_{p,c}$ = 0.40 V, ΔE = 120 mV).

The substitution of one DMSO ligand by a chlorido ligand in **2** shifts the potential by around 1000 mV to 0.05 V ($E_{p,a}$ = 0.1 V, $E_{p,c}$ = 0 V, ΔE = 100 mV) owing to the much higher electron-donating ability of the formally negatively charged chlorido ligand.

The cyclic voltammograms of **1a**, [**1a** – H]$^-$, and **1b** shown in Figure 4 and in the Supporting Information suggest the existence of a linkage isomerization process. With anodic scanning starting at 0 V for **1a**, a single anodic wave (i_{a1}) is observed at $E_{p,a}$ = 0.98 V. In the reverse segment, the corresponding i_{c1} cathodic wave ($E_{p,c}$ = 0.90 V) becomes less intense and a new cathodic wave (i_{c2}) at $E_{p,c}$ = 0.25 V appears. This effect gets more distinct with cathodic scanning starting at 1.4 V. This distinctive change in potential can be associated with the different coordination mode of a DMSO ligand, either S or O bound. Analogous observations were previously reported by Toma and coworkers.[22] The ratios of $[i_{c1}]/[i_{a1}]$ and $[i_{c2}]/[i_{a2}]$ strongly depend on the scan rate. This equilibrium upon one electron oxidation to Ru^{III} can be described as:

$$Ru^{III}-O \underset{k^{III}_{S\rightarrow O}}{\overset{k^{III}_{O\rightarrow S}}{\rightleftharpoons}} Ru^{III}-S \qquad \Big|\ K^{III}_{O\rightarrow S} \quad (2)$$

The equilibrium constant for the Ru^{III}–O/Ru^{III}–S reaction can be approximated from cyclic voltammograms starting at either 1.4 V for **1a** or 0.6 V for the deprotonated state [**1a** – H]$^-$. Plotting the ratio $[i_{c1}]/[i_{c2}]$ vs. v^{-1} and extrapolating $v \rightarrow \infty$ results in $K^{III}_{O\rightarrow S}$ = 0.27 (for **1a**) and $K^{III}_{O\rightarrow S}$ = 0.74 (for [**1a** – H]$^-$, see Supporting Information). The kinetic isomerization constants were calculated from the

© 2013 Wiley-VCH Verlag GmbH & Co. KGaA, Weinheim

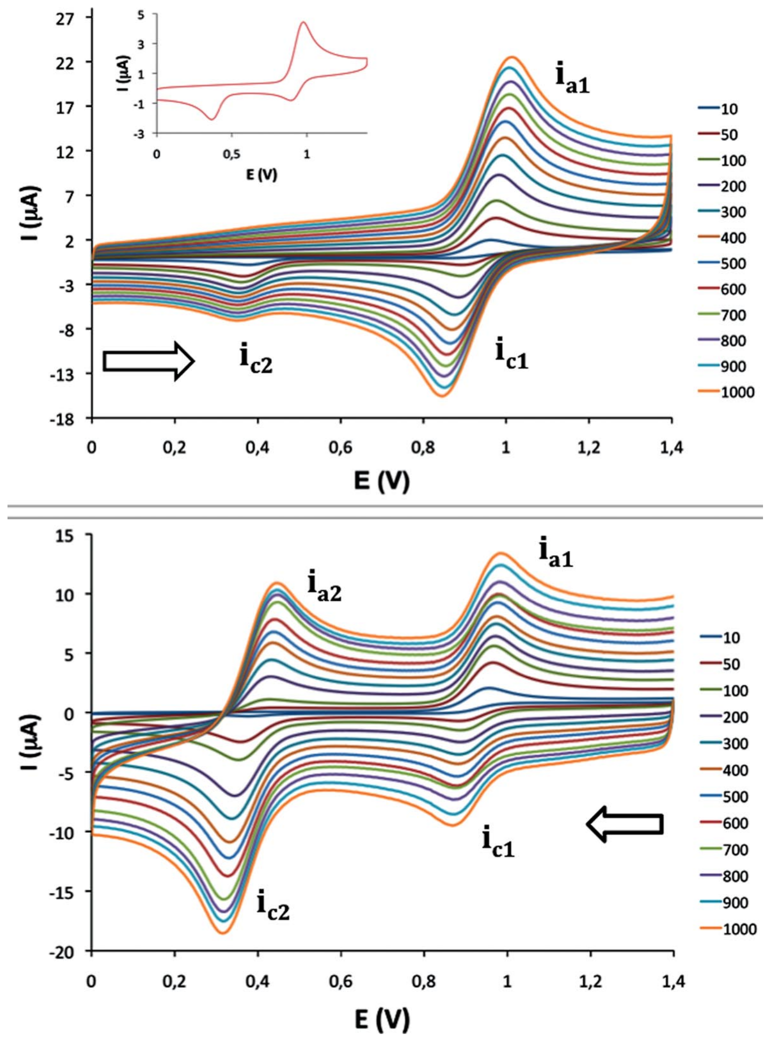

Figure 4. CV of **1a** in CH_2Cl_2/TBAH [(nBu$_4$N)(PF$_6$), 0.1 M] vs. SSCE starting from 0 V (top; inset shows CV at v = 50 mV/s) and from 1.4 V (bottom; applying E = 1.4 V for 1 min before scan). Arrow indicates initial scan direction; color code indicate scan rate in mV/s.

working curves proposed by Shain and coworkers[23] for a reversible chemical reaction preceding an electron transfer (case III; for more details on the calculation, see Formula section in the Supporting Information). The ratios i_k/i_d [i_k is the measured peak current (i_{c1}); i_d is the corresponding diffusion current in the absence of a chemical reaction (i_{a1})] were calculated by measuring i_k starting at 1.4 V (1 min QT) for **1a** and 0.6 V (1 min QT) (QT = quiet time, equilibration time) for [**1a** – H]$^-$ and i_d starting from 0 V (see Supporting Information). By calculating the equilibrium constant $K^{III}{}_{O\rightarrow S}$ and assuming that $E° = E_{1/2}$, the thermodynamic cycle shown in Scheme 3 can be derived and allows one to calculate $K^{II}{}_{O\rightarrow S}$.

The kinetic isomerization constants in the Ru^{II} oxidation state can be calculated from the dependency of $\ln(i_{a1}/v^{1/2})$ vs. time[22] (see Supporting Information) and the corresponding equation $K_{O\rightarrow S}{}^{II} = \dfrac{k_{O\rightarrow S}{}^{II}}{k_{S\rightarrow O}{}^{II}}$.

The same methodology was used to calculate the equilibrium and rate constants for **1b**, and the results obtained are summarized in Table 2.

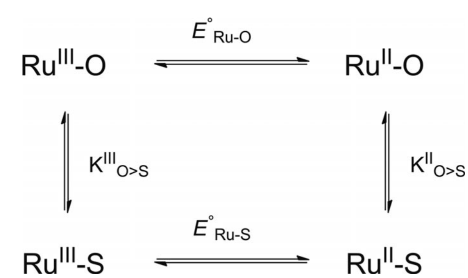

Scheme 3. Thermodynamic cycle for the isomerization process that occurs during electrochemical oxidation of **1a**, its deprotonated analog [**1a** – H]$^-$, and **1b**.

As can be seen from Table 2, in the Ru^{II} redox state in **1a** and its deprotonated analog [**1a** – H]$^-$, the DMSO ligand is dominantly bound to the metal center through the S atom. Upon oxidation to Ru^{III}, the DMSO ligand switches coordination from the S to the O atom. In both redox states deprotonation promotes the bonding of the DMSO ligand through the S atom. The change in potential suggests that only one DMSO ligand isomerizes during the electrochemi-

 © 2013 Wiley-VCH Verlag GmbH & Co. KGaA, Weinheim

Table 2. Thermodynamic and kinetic parameters for the linkage isomerization for **1a**, [**1a** – H]$^-$ and **1b** together with related Ru–DMSO complexes.

Compound	$K^{III}_{(O\to S)}$	$k^{III}_{O\to S}$ [s^{-1}]	$k^{III}_{S\to O}$ [s^{-1}]	$K^{II}_{(O\to S)}$	$k^{II}_{O\to S}$ [s^{-1}]	$k^{II}_{S\to O}$ [s^{-1}]	$E_1/_2$ (S) [V]	$E_1/_2$ (O) [V]
Toma et al.[22]	0.63	1.2	1.9	$2.1\times10^{+12}$	1.0×10^{-2}	5×10^{-14}	1.27[a]	0.55[a]
1a	2.7×10^{-1}	5.7×10^{-2}	2.2×10^{-1}	$5.3\times10^{+8}$	8.7×10^{-2}	1.6×10^{-10}	0.94[b]	0.39[b]
[**1a** – H]$^-$	7.4×10^{-1}	5.9×10^{-1}	8.0×10^{-1}	$1.5\times10^{+9}$	2.7×10^{-2}	1.8×10^{-11}	0.41[c]	–0.16[c]
1b	1.7	2.8×10^{-1}	1.7×10^{-1}	$5.2\times10^{+11}$	4.9×10^{-1}	9.3×10^{-14}	1.03[b]	0.46[b]
trans,cis-[Ru(Cl)$_2$(bpp)(DMSO)$_2$]$^-$ [21]	2.6×10^{-1}	1.7×10^{-2}	6.5×10^{-2}	$6.5\times10^{+9}$	1.3×10^{-1}	2.1×10^{-11}	0.38[c]	–0.20[c]
out-[Ru(L^2)(L^3)(DMSO)]$^+$ [15b]	1.3×10^{-1}	7.7×10^{-2}	6.0×10^{-1}	$5.5\times10^{+8}$	2.5×10^{-1}	4.6×10^{-10}	0.98[b]	0.41[b]
[Ru(L^1)(DMSO)]$^{2+}$ [15b]	1.7×10^{-3}	1.1×10^{-2}	6.5	$7.4\times10^{+7}$	3.6×10^{-2}	5.0×10^{-10}	1.24[b]	0.68[b]

[a] $E_{1/2}$ measured in MeCN/tetraethylammonium perchlorate (TEAP, 0.1 M). [b] $E_{1/2}$ measured in CH_2Cl_2/TBAH (0.1*M*). [c] $E_{1/2}$ measured in MeCN/TBAH (0.1 M). The acronym bpp stands for the 3,5-(2-pyridyl)pyrazolato ligand.

cal process. The second DMSO ligand, most likely the inner one, stays in its original coordination mode. Complex **1b** presents rather different behavior regarding this linkage isomerization. Though linkage isomerization is still observable upon oxidation, the dominant species is still the *S*-bound DMSO complex as the anodic scan shows $i_{a1} > i_{a2}$ (Figure S28, Supporting Information). This equilibrium is even further shifted upon deprotonation, as no linkage isomerization at all is observed for [**1b** – H]$^-$. This difference to its isomeric analogue is most likely due to a *trans* effect, as steric hindrance should be of comparable magnitude for both isomers.

Complex **2** shows no isomerization process during CV measurements (see Supporting Information). The high electron density on the metal center resulting from the three anionic chlorido ligands and the stabilizing effect of the described hydrogen bond explain this behavior. This result goes well with the findings for **1a** and **1b** and enables one to identify which DMSO ligand is performing the linkage isomerization.

Summary and Conclusions

The synthesis of two new isomeric Ru^{II} complexes containing the nonsymmetric chelating ligand H3p is described. Two isomers with the general formula [Ru(Cl)$_2$(H3p)(DMSO)$_2$] are thoroughly characterized through various techniques. For **1a**, the deprotonated analog [**1a** – H]$^-$, and **1b**, linkage isomerization of one of the coordinating DMSO ligand is investigated by cyclic voltammetric experiments. The differences in the behavior of the complexes in this process compared with previously reported complexes are highlighted. There is a strong dependency of the equilibrium constants and isomerization kinetics on the different ligand arrangements and electronic factors. Additionally, the light-induced substitution/oxidation reaction in $CHCl_3$ of both isomers to complex **2** was studied. The reaction is not initiated through UV-light induced bond homolysis of the solvent ($CHCl_3$), but rather implies high-energy π–π* transitions of the complexes themselves. Additionally, it could be shown that this reaction is oxygen independent. Complex **2** shows no linkage isomerization process, as in its oxidation state Ru^{III}, the DMSO ligand exclusively coordinates through its sulfur atom. We propose that this is due to the weakened Lewis acid character of the metal and stabilization through an existing intramolecular hydrogen bond.

Experimental Section

General Procedures: All reagents used in this work were obtained from Aldrich Chemical Co. and were used without further purification. Reagent grade organic solvents, CH_3CN (MeCN), CH_2Cl_2 and $(CH_3)_2SO$ (DMSO) were obtained from SDS and used as received. Chloroform ($CHCl_3$) and methanol (MeOH) were freshly distilled (basic alumina or Mg/I_2 respectively) before use. If not directly used, $CHCl_3$ was stored over basic alumina in amber glassware. NMR spectroscopic experiments were performed with a Bruker Avance 400 Ultrashield NMR spectrometer. Samples were dissolved in [D$_6$]DMSO with residual protons used as internal reference. Elemental analyses were performed with a CHNS-O EA-1108 elemental analyzer from Fisons. IR measurements were recorded with a Bruker Alpha FTIR spectrometer with an attenuated total reflectance (ATR) accessory. ESI mass spectra were recorded with a Waters LCT Premier Micromass spectrometer. UV/Vis spectroscopy was performed either with a Cary 50 (Varian) or a Tidas II (J&M) UV/Vis spectrophotometer with samples in 1 cm quartz cuvettes. Kinetic data treatment was performed with Specfit/32 from Spectrum Software Ass.[24]

Electrochemistry: Cyclic voltammetric (CV) experiments were performed with an IJ-Cambria HI-660 potentiostat using a three-electrode cell. A glassy carbon disk (2 mm Ø) or gold disk (1 mm Ø) was used as the working electrode, a platinum disk (1 mm Ø) as the auxiliary electrode, and an SSCE as the reference electrode. The working electrodes were thoughtfully polished with 0.05 micron alumina paste and were washed consecutively with distilled water and acetone followed by blow-drying before each measurement. Unless otherwise stated, all cyclic voltammograms presented in this work were recorded at a scan rate of 50 mV/s in the absence of light. The complexes were dissolved in CH_2Cl_2 or CH_3CN containing the necessary amount of TBAH [(nBu$_4$N)(PF$_6$)] as supporting electrolyte to yield a 0.1 M ionic strength solution.

Syntheses: *cis*-[Ru(Cl)$_2$(DMSO)$_4$][1] and the H3p[25] ligand were prepared according to literature procedures. All synthetic manipulations were routinely performed under an argon atmosphere by using Schlenk reaction vessels and vacuum line techniques. All spectroscopic and electrochemical experiments were performed in the absence of light unless explicitly mentioned.

***trans,cis*-[Ru(Cl)$_2$(H3p)(DMSO)$_2$] (1a):** A sample of [Ru(Cl)$_2$(DMSO)$_4$] (100 mg, 0.206 mmol) and H3p (46 mg, 0.206 mmol) were dissolved in freshly distilled MeOH (30 mL) and heated to reflux for 45 min under a static Ar atmosphere. The volume of the reaction was decreased until a precipitate formed. The yellow solid

 © 2013 Wiley-VCH Verlag GmbH & Co. KGaA, Weinheim

was removed by filtration, washed with Et_2O, and dried in vacuo, yield 79 mg (0.144 mmol, 70%). $C_{18}H_{23}Cl_2N_3O_2RuS_2·H_2O$: calcd. C 38.09, H 4.44, N 7.40, S 11.30; found C 38.37, H 4.14, N 7.36, S 11.32. ^1H NMR [300 MHz, $(CD_3)_2SO$, 25 °C]: δ = 8.81 (d, ^3J = 5.6 Hz, 1 H, 1-H), 8.26 (d, ^3J = 7.7 Hz, 1 H, 4-H), 8.15 (t, ^3J = 7.7 Hz, 1 H, 3-H), 7.8 (d, ^3J = 1.8 Hz, 1 H, 7-H), 7.73 (d, ^3J = 7.7 Hz, 2 H, 14-H, 10-H), 7.59 (t, ^3J = 7.7 Hz, 2 H, 13-H, 11-H), 7.54 (t, ^3J = 6.4 Hz, 1 H, 2-H), 7.49 (t, ^3J = 7.3 Hz, 1 H, 12-H), 3.48 (s, 6 H), 3.44 (s, 6 H) ppm. $^{13}C\{^1H\}$ NMR [100 MHz, $(CD_3)_2SO$, 25 °C]: δ = 153.8, 152.3, 151.6, 144.0, 139.2, 130.2, 127.9, 125.2, 122.2, 102.1, 44.6, 43.1 ppm. ESI-MS (MeOH): m/z = 574.0 $[M + Na]^+$. UV/Vis ($CHCl_3$): λ_{max} (ε, $M^{-1}cm^{-1}$) = 253 (22230), 290 (21970), 385 (3040) nm. CV (vs. SSCE): $E_{1/2}^{III/II}$ (S-DMSO) = 0.94 V; ΔE = 80 mV [CH_2Cl_2/TBAH (0.1 M)], $E_{1/2}^{III/II}$ (O-DMSO) = 0.39 V; ΔE = 60 mV [CH_2Cl_2/TBAH (0.1 M)], $E_{1/2}^{III/II}$ (S-DMSO) = 0.28 V; ΔE = 60 mV [CH_2Cl_2/TBAH (0.1 M)/NaO*t*Bu], $E_{1/2}^{III/II}$ (O-DMSO) = –0.27 V; ΔE = 80 mV [CH_2Cl_2/TBAH (0.1 M)/NaO*t*Bu], $E_{1/2}^{III/II}$ (S-DMSO) = 0.41 V; ΔE = 60 mV [MeCN/TBAH (0.1 M)/NaO*t*Bu], $E_{1/2}^{III/II}$ (O-DMSO) = –0.16 V; ΔE = 80 mV [MeCN-TBAH (0.1 M)/NaO*t*Bu].

***cis*(*out*),*cis*(*in*)-[Ru(Cl)$_2$(H3p)(DMSO)$_2$] (1b):** The same procedure as for **1a** was used with the reaction time extended to 18 h, yield 85 mg [0.155 mmol (75%)]. $C_{18}H_{23}Cl_2N_3O_2RuS_2·2H_2O$: calcd. C 36.92, H 4.65, N 7.18, S 10.95; found C 36.77, H 4.33, N 7.03, S 10.86. ^1H NMR [300 MHz, $(CD_3)_2SO$, 25 °C]: δ = 9.29 (d, ^3J = 5.7 Hz, 1 H, 1-H), 8.26 (t, ^3J = 7.6 Hz, 1 H, 4-H), 8.22 (t, ^3J = 7.6 Hz, 1 H, 3-H), 7.81 (s, 1 H, 7-H), 7.71 (m, 3 H, 14-H, 10-H, 2-H), 7.58 (t, ^3J = 7.5 Hz, 2 H, 13-H, 11-H), 7.49 (t, ^3J = 7.3 Hz, 1 H, 12-H), 3.51 (s, 3 H), 3.49 (s, 3 H), 2.96 (s, 3 H), 2.21 (s, 3 H) ppm. $^{13}C\{^1H\}$ NMR [100 MHz, $(CD_3)_2SO$, 25 °C]: δ = 152.8, 152.1, 151.9, 145.3, 139.3, 130.1, 127.5, 125.4, 122.3, 103.0, 45.5, 45.0, 44.9, 43.7 ppm. ESI-MS (MeOH): m/z = 574.0 $[M + Na]^+$. UV/Vis ($CHCl_3$): λ_{max} (ε, $M^{-1}cm^{-1}$) = 277 (18920), 292 (19500), 415 (1990) nm. CV (vs. SSCE): $E_{1/2}^{III/II}$ (S-DMSO) = 1.03 V; ΔE = 60 mV [CH_2Cl_2/TBAH (0.1 M)], $E_{1/2}^{III/II}$ (S-DMSO) = 0.46 V; ΔE = 120 mV [CH_2Cl_2-TBAH (0.1 M)/NaO*t*Bu].

***in*-[Ru(Cl)$_3$(H3p)(DMSO)] (2):** This compound was isolated after overnight irradiation of solutions of either **1a** or **1b** in $CHCl_3$ with light (200 W Tungsten lamp). Evaporation of the solvent, washing the solid with Et_2O, and drying it in vacuo produced **2** in quantitative yield. $C_{16}H_{17}Cl_3N_3ORuS·0.4H_2O$: calcd. C 37.39, H 3.49, N 8.17, S 6.24; found C 37.59, H 3.28, N 7.99, S 5.98. ESI-MS (MeOH): m/z = 507.8 $[M]^-$, 471.0 $[M – Cl]^-$, 429.8 $[M – DMSO]^-$. UV/Vis ($CHCl_3$): λ_{max} (ε, $M^{-1}cm^{-1}$) = 277 (18200), 341 (3350), 405 (5250), 462 (3500), 565 (1500). CV (vs. SSCE): $E_{1/2}^{III/II}$ (S-DMSO) = 0.05 V; ΔE = 80 mV [CH_2Cl_2/TBAH (0.1 M)].

X-ray Crystal Structure Determination: Suitable crystals of *trans,cis*-[Ru(Cl)$_2$(H3p)(DMSO)$_2$] (**1a**), *cis(out),cis(in)*-[Ru(Cl)$_2$(H3p)(DMSO)$_2$] (**1b**), and *in*-[Ru(Cl)$_3$(H3p)(DMSO)] (**2**) were obtained from slow diffusion of ethyl ether into a saturated solution of each complex in $CHCl_3$. The crystals were prepared under inert conditions and were immersed in perfluoropolyether as protecting oil for manipulation.

Data Collection: The crystal structure determinations for **1b** and **2** were performed with a Bruker-Nonius diffractometer equipped with an APPEX 2 4 K CCD area detector, a FR591 rotating anode with Mo-K_α radiation, Montel mirrors as monochromator, and an Oxford Cryosystems low-temperature device Cryostream 700 plus (T = –173 °C). The crystal structure determination for **1a** was performed with an Apex DUO Kappa 4-axis goniometer equipped with an APPEX 2 4K CCD area detector, a Microfocus Source E025 IuS using Mo-K_α radiation, Quazar MX multilayer Optics as monochromator, and an Oxford Cryosystems low temperature device Cryostream 700 plus (T = –173 °C). Full-sphere data collection was used with ω and ϕ scans. Programs used: Data collection APEX-2,[26] data reduction Bruker Saint[27] version 7.60A, and absorption correction SADABS.[28]

Structure Solution and Refinement: Crystal structure solution was achieved by using direct methods as implemented in SHELXTL[29] and structures were visualized using the program XP. Missing atoms were subsequently located from difference Fourier synthesis and were added to the atom list. Least-squares refinement on F^2 using all measured intensities was carried out using the program SHELXTL. All non-hydrogen atoms were refined with anisotropic displacement parameters. The crystals of compound **1b** were mostly twinned, and after several attempts a crystal suitable for structure determination could be obtained. Probably, owing to the presence of a second small crystal, the ellipsoids of the structure show some distortion and the R_1 value could be only lowered to 8.03%. This structure is a chloroform solvate. The chloroform molecule is disordered in two orientations (ratio 52:48). Compound **1a** crystallizes as a racemic twin (BASF 0.35) and is pseudo-centrosymmetric with two independent molecules of the complex in the asymmetric unit. Refinement in the space group $C2/c$ could only lower the R_1 value to 18%, thus the space group Cc was selected (R_1 = 4.44%). Probably, owing to the pseudo-centrosymmetry, some nonexpected electron densities were observed in nonsensical positions and were not refined. This structure is a chloroform solvate. Compound **2** is also a chloroform solvate.

CCDC-903111, -903112, and -903113 contain the supplementary crystallographic data for this paper. These data can be obtained free of charge from The Cambridge Crystallographic Data Centre via www.ccdc.cam.ac.uk/data_request/cif

Supporting Information (see footnote on the first page of this article): UV/Vis and NMR spectra, cyclic voltammograms, and crystallographic data.

Acknowledgments

Support from SOLAR-H2 (EU 212508), Ministerio de Ciencia e Innovación (MICINN) (CTQ2007-67918, CTQ2010-21497), and Consolider Ingenio 2010 (CSD2006-0003) are gratefully acknowledged. S. R. is grateful for the award of doctoral grant from MICINN.

[1] I. P. Evans, A. Spencer, G. Wilkinson, *J. Chem. Soc., Dalton Trans.* **1973**, 204–209.

[2] a) G. Sava, E. Alessio, A. Bergamo, G. Mestroni, *Topics in Biological Inorganic Chemistry*, vol. 1, *Metallo-Pharmaceuticals*, Springer, Berlin, **1999**; b) E. Alessio, G. Mestroni, A. Bergamo, G. Sava, in: *Metal Ions in Biological Systems*, vol. 42, *Metal Complexes in Tumor Diagnosis and as Anticancer Agents* (Eds.: A. Sigel, H. Sigel), Dekker, New York, **2004**, chapter 10; c) C. Tan, J. Liu, L. Chen, S. Shi, L. Ji, *J. Inorg. Biochem.* **2008**, *102*, 1644–1653.

[3] P. K. L. Chan, P. K. H. Chan, D. C. Frost, B. R. James, K. A. Skov, *Can. J. Chem.* **1988**, *66*, 117–122.

[4] a) D. P. Riley, *Inorg. Chem.* **1983**, *22*, 1965–1967; b) D. P. Riley, M. R. Thompson, J. Lyon, *J. Coord. Chem.* **1988**, *19*, 49–59; c) R. S. Srivastava, *Appl. Organomet. Chem.* **2001**, *15*, 769–771.

[5] a) J. Trocha-Grimshaw, H. B. Henbest, *Chem. Commun. (London)* **1968**, 1035; b) J. Trocha-Grimshaw, H. B. Henbest, *J. Chem. Soc. Perkin Trans. 1* **1974**, *1*, 607.

[6] S. N. Gamage, B. R. James, *J. Chem. Soc., Chem. Commun.* **1989**, 1624–1626.

 © 2013 Wiley-VCH Verlag GmbH & Co. KGaA, Weinheim

[7] N. N. Dass, S. R. Sen, *J. Polym. Sci. Polym. Chem. Ed.* **1983**, *21*, 3381–3388.
[8] R. Castarlenas, I. Alaoui-Abdallaoui, D. Semeril, B. Mernari, S. Guesmi, P. H. Dixneuf, *New J. Chem.* **2003**, *27*, 6–8.
[9] R. C. van der Drift, J. W. Sprengers, E. Bouwman, W. P. Mul, H. Kooijman, A. L. Spek, E. Drent, *Eur. J. Inorg. Chem.* **2002**, 2147–2155.
[10] a) J. J. Rack, J. R. Winkler, H. B. Gray, *J. Am. Chem. Soc.* **2001**, *123*, 2432–2433; b) A. A. Rachford, J. L. Petersen, J. J. Rack, *Inorg. Chem.* **2005**, *44*, 8065–8075.
[11] a) A. Yeh, N. Scott, H. Taube, *Inorg. Chem.* **1982**, *21*, 2542–2545; b) M. Sano, H. Taube, *Inorg. Chem.* **1994**, *33*, 705–709.
[12] a) C. P. Collier, E. W. Wong, Belohradsk, M. Yacute, F. M. Raymo, J. F. Stoddart, P. J. Kuekes, R. S. Williams, J. R. Heath, *Science* **1999**, *285*, 391–394; b) S. Bonnet, J.-P. Collin, M. Koizumi, P. Mobian, J.-P. Sauvage, *Adv. Mater.* **2006**, *18*, 1239–1250.
[13] a) A. P. d. Silva, N. D. McClenaghan, *Chem. Eur. J.* **2004**, *10*, 574–586; b) J. J. Rack, *Coord. Chem. Rev.* **2009**, *253*, 78–85.
[14] P. E. Hoggard, *J. Coord. Chem.* **2009**, *62*, 1743–1753.
[15] a) J. Mola, I. Romero, M. Rodriguez, F. Bozoglian, A. Poater, M. Sola, T. Parella, J. Benet-Buchholz, X. Fontrodona, A. Llobet, *Inorg. Chem.* **2007**, *46*, 10707–10716; b) J. Benet-Buchholz, P. Comba, A. Llobet, S. Roeser, P. Vadivelu, S. Wiesner, *Dalton Trans.* **2010**, *39*, 3315–3320.
[16] M. Calligaris, O. Carugo, *Coord. Chem. Rev.* **1996**, *153*, 83–154.
[17] T. Steiner, *Angew. Chem.* **2002**, *114*, 50–80.
[18] S. Roeser, P. Farràs, F. Bozoglian, M. Martínez-Belmonte, J. Benet-Buchholz, A. Llobet, *ChemSusChem* **2011**, *4*, 197–207.
[19] B. Serli, E. Zangrando, T. Gianferrara, L. Yellowlees, E. Alessio, *Coord. Chem. Rev.* **2003**, *245*, 73–83.
[20] a) S. Geremia, E. Alessio, F. Todone, *Inorg. Chim. Acta* **1996**, *253*, 87–90; b) J. J. Rack, H. B. Gray, *Inorg. Chem.* **1998**, *37*, 2–3.
[21] C. Sens, M. Rodriguez, I. Romero, A. Llobet, T. Parella, B. P. Sullivan, J. Benet-Buchholz, *Inorg. Chem.* **2003**, *42*, 2040–2048.
[22] D. O. Silva, H. E. Toma, *Can. J. Chem.* **1994**, *72*, 1705–1708.
[23] R. S. Nicholson, I. Shain, *Anal. Chem.* **1964**, *36*, 706–723.
[24] G. A. Kriss, *A S. P. Conf., Ser.* **1994**, *61*, 437.
[25] A. Chadghan, J. Pons, A. Caubet, J. Casabo, J. Ros, A. Alvarez-Larena, J. F. Piniella, *Polyhedron* **2000**, *19*, 855–862.
[26] *Data collection with APEX II*, v.1.0-22, v.2009.1-0, and v.2009.1-02, Bruker AXS Inc., Madison, Wisconsin, USA, **2007**.
[27] *Data reduction with Bruker SAINT*, v.2.2.10(2003) and v.7.60A, Bruker AXS Inc., Madison, Wisconsin, USA, **2007**.
[28] a) *SADABS*, v.2.10(2003), v.2008, and v.2008/1, Bruker AXS, Inc., Madison, Wisconsin, USA, **2001**; b) Blessing, *Acta Crystallogr., Sect. A* **1995**, *51*, 33–38.
[29] G. M. Sheldrick, *Acta Crystallogr., Sect. A* **2008**, *64*, 112–122.

Received: July 16, 2012
Published Online: November 21, 2012

 © 2013 Wiley-VCH Verlag GmbH & Co. KGaA, Weinheim